Model order reduction based solver for discontinuous Galerkin element approximation of time-domain Maxwell's equations in dispersive media

Kun Li, Ting-Zhu Huang, Liang Li, Stephane Lanteri

Model order reduction based solver for discontinuous Galerkin element approximation of time-domain Maxwell's equations in dispersive media

Kun Li[1], Ting-Zhu Huang[1], Liang Li[1] Stéphane Lanteri[2]

[1]School of Mathematical Sciences, UESTC, P.R. China
[2]INRIA, 2004 Route des Lucioles, BP 93 06902 Sophia Antipolis Cedex, France

20th IMACS WORLD CONGRESS,
10-14 December 2016.

Outline

1. Introduction
   - Model Problem
   - Motivation
   - Model order reduction
2. DGTD formulations
   - Weak variation
   - Space-discrete formulation
3. Reduced-order DG formulations
   - POD-DGTD formulations
   - Krylov subspace based solver
     - Krylov-subspace based operator exponential approach
     - Krylov-subspace based Padé approximation approach
4. Numerical experiments
   - Artificial validation case
   - Scattering of a plane wave by a Au-nanowire
5. Summary

Outline

1 Introduction
- Model Problem
- Motivation
- Model order reduction

2 DGTD formulations
- Weak variation
- Space-discrete formulation

3 Reduced-order DG formulations
- POD-DGTD formulations
- Krylov subspace based solver
  - Krylov-subspace based operator exponential approach
  - Krylov-subspace based Padé approximation approach

4 Numerical experiments
- Artificial validation case
- Scattering of a plane wave by a Au-nanowire

5 Summary

Time-domain Maxwell-Drude equations

$$
\begin{cases}
\frac{\partial \mathbf{H}}{\partial t} + \mathrm{curl}\mathbf{E} = 0 \ \text{ in } \Omega \times (0, t_f], \\
\varepsilon_\infty \frac{\partial \mathbf{E}}{\partial t} - \mathrm{curl}\mathbf{H} + \mathbf{J} = 0 \ \text{ in } \Omega \times (0, t_f], \\
\frac{\partial \mathbf{J}}{\partial t} + \gamma_d \mathbf{J} - \omega_d^2 \mathbf{E} = 0 \ \text{ in } \Omega_s \times (0, t_f], \\
\mathbf{E}(\mathbf{x}; 0) = \mathbf{E}_0(\mathbf{x}), \mathbf{H}(\mathbf{x}; 0) = \mathbf{H}_0(\mathbf{x}) \ \text{ in } \Omega, \\
\mathbf{J}(\mathbf{x}; 0) = \mathbf{J}_0(\mathbf{x}) \ \text{ in } \Omega_s.
\end{cases} \tag{1}
$$

Time-domain Maxwell-Drude equations

$$
\begin{cases}
\dfrac{\partial \mathbf{H}}{\partial t} + \operatorname{curl}\mathbf{E} = 0 \ \text{ in } \Omega \times (0, t_f], \\
\varepsilon_\infty \dfrac{\partial \mathbf{E}}{\partial t} - \operatorname{curl}\mathbf{H} + \mathbf{J} = 0 \ \text{ in } \Omega \times (0, t_f], \\
\dfrac{\partial \mathbf{J}}{\partial t} + \gamma_d \mathbf{J} - \omega_d^2 \mathbf{E} = 0 \ \text{ in } \Omega_s \times (0, t_f], \\
\mathbf{E}(\mathbf{x}; 0) = \mathbf{E}_0(\mathbf{x}), \mathbf{H}(\mathbf{x}; 0) = \mathbf{H}_0(\mathbf{x}) \ \text{ in } \Omega, \\
\mathbf{J}(\mathbf{x}; 0) = \mathbf{J}_0(\mathbf{x}) \ \text{ in } \Omega_s.
\end{cases} \tag{1}
$$

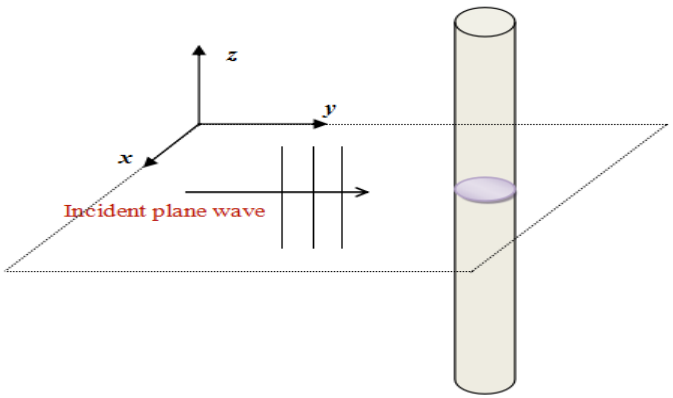

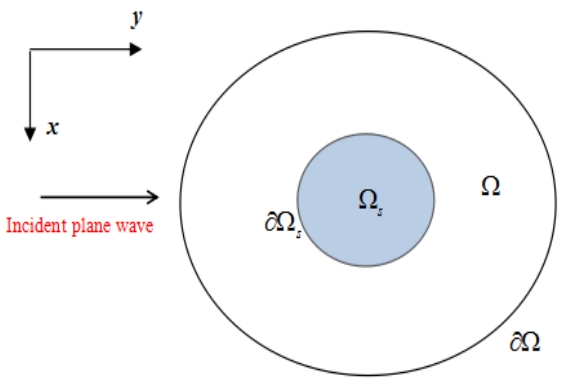

Time-domain Maxwell-Drude equations

$$\begin{cases} \frac{\partial \mathbf{H}}{\partial t} + \mathrm{curl}\mathbf{E} = 0 \ \text{ in } \Omega \times (0, t_f], \\ \varepsilon_\infty \frac{\partial \mathbf{E}}{\partial t} - \mathrm{curl}\mathbf{H} + \mathbf{J} = 0 \ \text{ in } \Omega \times (0, t_f], \\ \frac{\partial \mathbf{J}}{\partial t} + \gamma_d \mathbf{J} - \omega_d^2 \mathbf{E} = 0 \ \text{ in } \Omega_s \times (0, t_f], \\ \mathbf{E}(\mathbf{x}; 0) = \mathbf{E}_0(\mathbf{x}), \mathbf{H}(\mathbf{x}; 0) = \mathbf{H}_0(\mathbf{x}) \ \text{ in } \Omega, \\ \mathbf{J}(\mathbf{x}; 0) = \mathbf{J}_0(\mathbf{x}) \ \text{ in } \Omega_s. \end{cases} \tag{1}$$

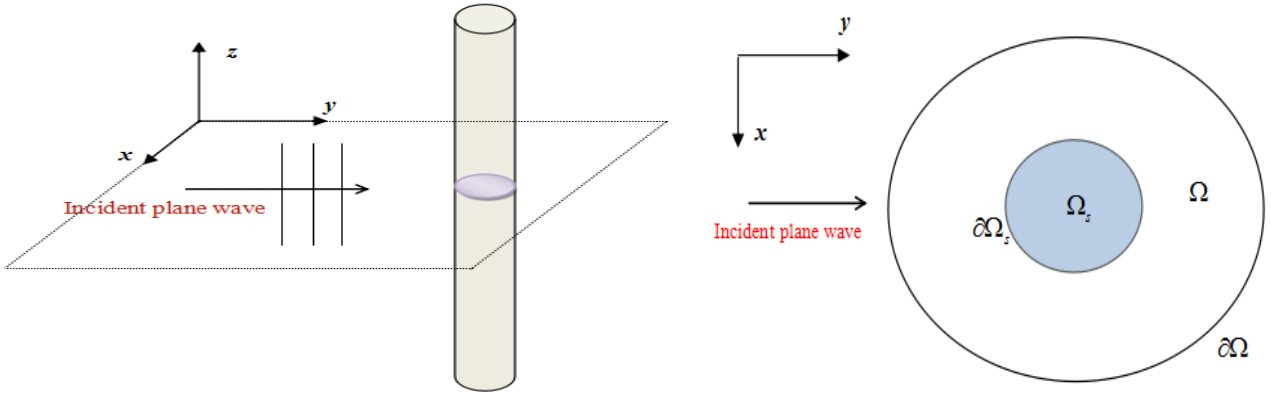

- $\Omega \in \mathbb{R}^d$, $d = 2, 3$, t_f is the final physical time.
- **E**, **H**, and **J** respectively denote the electric field, the magnetic field and the dipolar current vector.

Boundary condition

Hard-wall condition [Schmitt N, Scheid C, Lanteri S, et al, JCP, 2016.]:

$$\mathbf{n} \cdot \mathbf{J} = 0 \quad \text{on } \partial\Omega_s. \tag{2}$$

Perfect electric conductor condition (PEC):

$$\mathbf{n} \times \mathbf{E} = 0 \quad \text{on } \Gamma_m. \tag{3}$$

First order Silver-Müller absorbing boundary condition (ABC):

$$\mathbf{n} \times \mathbf{E} + z\mathbf{n} \times (\mathbf{n} \times \mathbf{H}) = \mathbf{n} \times \mathbf{E}^{inc} + z\mathbf{n} \times (\mathbf{n} \times \mathbf{H}^{inc}) \quad \text{on } \Gamma_a. \tag{4}$$

Boundary condition

Hard-wall condition [Schmitt N, Scheid C, Lanteri S, et al, JCP, 2016.]:

$$\mathbf{n} \cdot \mathbf{J} = 0 \quad \text{on } \partial\Omega_s. \tag{2}$$

Perfect electric conductor condition (PEC):

$$\mathbf{n} \times \mathbf{E} = 0 \quad \text{on } \Gamma_m. \tag{3}$$

First order Silver-Müller absorbing boundary condition (ABC):

$$\mathbf{n} \times \mathbf{E} + z\mathbf{n} \times (\mathbf{n} \times \mathbf{H}) = \mathbf{n} \times \mathbf{E}^{inc} + z\mathbf{n} \times (\mathbf{n} \times \mathbf{H}^{inc}) \quad \text{on } \Gamma_a. \tag{4}$$

- $\Gamma_m \cap \Gamma_a = \varnothing$, $\Gamma_m \cup \Gamma_a = \partial\Omega$, $\varnothing$ is an empty set.
- $\mathbf{n}$ denotes the unit normal vector pointing outward to $\partial\Omega$.
- $\mathbf{E}^{inc}$ and $\mathbf{H}^{inc}$ are the incident fields.
- $z = \sqrt{\mu/\varepsilon}$.

Outline

1 Introduction
- Model Problem
- Motivation
- Model order reduction

2 DGTD formulations
- Weak variation
- Space-discrete formulation

3 Reduced-order DG formulations
- POD-DGTD formulations
- Krylov subspace based solver
  - Krylov-subspace based operator exponential approach
  - Krylov-subspace based Padé approximation approach

4 Numerical experiments
- Artificial validation case
- Scattering of a plane wave by a Au-nanowire

5 Summary

Motivation

At present, most of numerical solvers for (1) with (2)-(4) can be summarized as: FDTD, FETD, FVTD, DGTD, etc. The DGTD methods has many advantages compared with the previous numerical methods:

- the use of unstructured possibly non-conforming meshes.
- easily obtained high order accuracy.
- *hp* -adaptivity.
- natural parallelism.
- ...

Motivation

DOFs of the DGTD method: $N_{dof} = \sum_{i=1}^{n_t} d_i$.

- n_t is the number of elements.
- d_i is the number of DOFs on element i.
  - 1D: $d_i = p + 1$.
  - 2D: $d_i = \frac{1}{2}(p+1)(p+2)$.
  - 3D: $d_i = \frac{1}{6}(p+1)(p+2)(p+3)$.

Motivation

DOFs of the DGTD method: $N_{dof} = \sum_{i=1}^{n_t} d_i$.

- n_t is the number of elements.
- d_i is the number of DOFs on element i.
  - 1D: $d_i = p + 1$.
  - 2D: $d_i = \frac{1}{2}(p+1)(p+2)$.
  - 3D: $d_i = \frac{1}{6}(p+1)(p+2)(p+3)$.

Thus, it becomes an important problem how to get a low dimensional system that has the same response characteristics as the original system, while

- sufficiently accurate numerical solutions.
- far less storage requirements and much lower evaluation time.

Outline

1 Introduction
- Model Problem
- Motivation
- Model order reduction

2 DGTD formulations
- Weak variation
- Space-discrete formulation

3 Reduced-order DG formulations
- POD-DGTD formulations
- Krylov subspace based solver
  - Krylov-subspace based operator exponential approach
  - Krylov-subspace based Padé approximation approach

4 Numerical experiments
- Artificial validation case
- Scattering of a plane wave by a Au-nanowire

5 Summary

MOR

- Proper orthogonal decomposition (POD) methods [Holmes P, Lumley J L, Berkooz G, 1998].
- Krylov subspaces methods.
  - Padé-via-Lanczos (PVL) [R Freund, P Feldmann, 1993].
  - the Arnoldi method.
  - the multi-point rational Krylov subspaces [K Gallivan, E Grimme, 1996].
  - ...
- Balanced truncation methods [Moore B, 1981]
- ...

Notations

- K_i: an element of the mesh.
- N_Ω: the set of indices of the mesh elements.
- F_h^I: the union of all interior interfaces.
- F_h^B: the union of all boundary interfaces.
- F_{ij}: the common face of the K_i and K_j, K_j is a adjacent element.
- $\nu_i := \{j | K_i \cap K_j \neq \varnothing\}$: the set of indices of the elements which are neighbors of K_i.

Notations

- K_i: an element of the mesh.
- N_Ω: the set of indices of the mesh elements.
- F_h^I: the union of all interior interfaces.
- F_h^B: the union of all boundary interfaces.
- F_{ij}: the common face of the K_i and K_j, K_j is a adjacent element.
- $\nu_i := \{j | K_i \cap K_j \neq \varnothing\}$: the set of indices of the elements which are neighbors of K_i.

For a face $F_{ij} \in F_h^I$, we define average values $\{\cdot\}$:

$$\{\mathbf{v}\}_{F_{ij}} = \frac{1}{2}(\mathbf{v}_j + \mathbf{v}_i)$$

where $\mathbf{v}_j$ and $\mathbf{v}_i$ respectively stand for the traces of $\mathbf{v}$ on F_{ij} from the interior of K_j and K_i. The finite dimensional subspace can be defined by:

$$\mathbf{V}_h^p := \{\mathbf{v} \in (L^2(\Omega))^3 \mid \mathbf{v}_{|K_i} \in (\mathbb{P}_p(K_i))^3, \quad \forall i \in N_\Omega\}.$$

The restrictions of $\mathbf{V}_h^p$ in Ω_s is denoted by $\widetilde{\mathbf{V}}_h^p$.

Outline

1 Introduction
- Model Problem
- Motivation
- Model order reduction

2 DGTD formulations
- Weak variation
- Space-discrete formulation

3 Reduced-order DG formulations
- POD-DGTD formulations
- Krylov subspace based solver
  - Krylov-subspace based operator exponential approach
  - Krylov-subspace based Padé approximation approach

4 Numerical experiments
- Artificial validation case
- Scattering of a plane wave by a Au-nanowire

5 Summary

Weak variation

The DG method seeks an approximate solution $(\mathbf{E}_h, \mathbf{H}_h, \mathbf{J}_h)$ in the space $\mathbf{V}_h^p \times \mathbf{V}_h^p \times \widetilde{\mathbf{V}}_h^p$ that should satisfy for all K_i in Ω_h:

$$\begin{cases} (\frac{\partial \mathbf{H}_h}{\partial t}, \mathbf{v})_{K_i} + (\mathrm{curl}\mathbf{E}_h, \mathbf{v})_{K_i} = 0, \quad \forall \mathbf{v} \in \mathbf{V}_h^p, \\ (\varepsilon_\infty \frac{\partial \mathbf{E}_h}{\partial t}, \mathbf{v})_{K_i} - (\mathrm{curl}\mathbf{H}_h, \mathbf{v})_{K_i} + (\mathbf{J}_h, \mathbf{v})_{K_i} = 0, \quad \forall \mathbf{v} \in \mathbf{V}_h^p, \\ (\frac{\partial \mathbf{J}_h}{\partial t}, \mathbf{v})_{K_i} + (\gamma_d \mathbf{J}_h, \mathbf{v})_{K_i} - (\omega_d^2 \mathbf{E}_h, \mathbf{v})_{K_i} = 0, \quad \forall \mathbf{v} \in \widetilde{\mathbf{V}}_h^p. \end{cases} \tag{5}$$

Using appropriate Green's formulas and replacing the boundary terms by numerical traces $\mathbf{E}_h^*$ and $\mathbf{H}_h^*$ in (5), which are also known as numerical fluxes, we have:

$$\begin{cases} (\frac{\partial \mathbf{H}_h}{\partial t}, \mathbf{v})_{K_i} + (\mathbf{E}_h, \mathrm{curl}\mathbf{v})_{K_i} - \langle \mathbf{E}_h^* \times \mathbf{n}, \mathbf{v} \rangle_{\partial K_i} = 0 \quad \forall \mathbf{v} \in \mathbf{V}_h^p, \\ (\varepsilon_\infty \frac{\partial \mathbf{E}_h}{\partial t}, \mathbf{v})_{K_i} - (\mathbf{H}_h, \mathrm{curl}\mathbf{v})_{K_i} + (\mathbf{J}_h, \mathbf{v})_{K_i} + \langle \mathbf{H}_h^* \times \mathbf{n}, \mathbf{v} \rangle_{\partial K_i} = 0 \quad \forall \mathbf{v} \in \mathbf{V}_h^p, \\ (\frac{\partial \mathbf{J}_h}{\partial t}, \mathbf{v})_{K_i} + (\gamma_d \mathbf{J}_h, \mathbf{v})_{K_i} - (\omega_d^2 \mathbf{E}_h, \mathbf{v})_{K_i} = 0 \quad \forall \mathbf{v} \in \widetilde{\mathbf{V}}_h^p. \end{cases}$$

Outline

1 Introduction
- Model Problem
- Motivation
- Model order reduction

2 DGTD formulations
- Weak variation
- Space-discrete formulation

3 Reduced-order DG formulations
- POD-DGTD formulations
- Krylov subspace based solver
  - Krylov-subspace based operator exponential approach
  - Krylov-subspace based Padé approximation approach

4 Numerical experiments
- Artificial validation case
- Scattering of a plane wave by a Au-nanowire

5 Summary

Space-discrete formulation

Proper choice of numerical traces $\mathbf{E}_h^*$ and $\mathbf{H}_h^*$ is essential for the correctness and the convergence of the scheme. For the sake of simplicity, we choose to use a fully centered numerical flux, i.e.

$$\mathbf{E}_h^* = \{\mathbf{E}_h\}_{F_{ij}}, \quad \mathbf{H}_h^* = \{\mathbf{H}_h\}_{F_{ij}}, \quad \forall i \in N_\Omega, \ \forall j \in \nu_i.$$

Replacing surface integrals using centered fluxes in (6) and, re-integrating by parts yields:

$$\begin{cases} (\frac{\partial \mathbf{H}_h}{\partial t}, \mathbf{v})_{K_i} = -\frac{1}{2}((\mathrm{curl}\mathbf{v}, \mathbf{E}_h)_{K_i} + (\mathrm{curl}\mathbf{E}_h, \mathbf{v})_{K_i}) + \frac{1}{2}\sum_{l\in\nu_i} \langle \mathbf{E}_l \times \mathbf{n}, \mathbf{v}\rangle_{F_{il}}, \\ (\varepsilon_\infty \frac{\partial \mathbf{E}_h}{\partial t}, \mathbf{v})_{K_i} = \frac{1}{2}((\mathrm{curl}\mathbf{v}, \mathbf{H}_h)_{K_i} + (\mathrm{curl}\mathbf{H}_h, \mathbf{v})_{K_i}) - \frac{1}{2}\sum_{l\in\nu_i} \langle \mathbf{H}_l \times \mathbf{n}, \mathbf{v}\rangle_{F_{il}}, \\ (\frac{\partial \mathbf{J}_h}{\partial t}, \mathbf{v})_{K_i} = -(\gamma_d \mathbf{J}_h, \mathbf{v})_{K_i} + (\omega_d^2 \mathbf{E}_h, \mathbf{v})_{K_i}. \end{cases} \tag{7}$$

Space-discrete formulation

We now define a set of scalar basis functions φ_{ik} $(1 \leq k \leq d_i)$ on the element K_i, and then vectorize the basis functions (as well as the test functions), so in a 3D setting we have $\forall i \in N_\Omega$, $0 \leq k \leq d_i$, the vectorial basis functions

$$\Phi_{ik}^1 = (\varphi_{ik}, 0, 0)^T, \ \Phi_{ik}^2 = (0, \varphi_{ik}, 0)^T \text{and } \Phi_{ik}^3 = (0, 0, \varphi_{ik})^T.$$

The test function $\mathbf{v}$ can be chosen as the $3d_i$ vectors Φ_{ik}^m $(1 \leq k \leq d_i,$ $1 \leq m \leq 3)$. Then the problem (7) can be denoted by an equivalent matrix form:

$$\begin{cases} \mathbb{M}_i \frac{d\underline{\mathbf{H}}_i}{dt} = -\mathbb{K}_i \underline{\mathbf{E}}_i + \sum_{l \in \nu_i} \mathbb{S}_{il} \underline{\mathbf{E}}_l, \\ \varepsilon_\infty \mathbb{M}_i \frac{d\underline{\mathbf{E}}_i}{dt} = \mathbb{K}_i \underline{\mathbf{H}}_i - \mathbb{M}_i \underline{\mathbf{J}}_i - \sum_{l \in \nu_i} \mathbb{S}_{il} \underline{\mathbf{H}}_l, \\ \frac{d\underline{\mathbf{J}}_i}{dt} = -\gamma_d \underline{\mathbf{J}}_i + \omega_d^2 \underline{\mathbf{E}}_i. \end{cases} \tag{8}$$

Space-discrete formulation

Here, the 3×3 block diagonal mass matrix $\mathbb{M}_i$, the 3×3 block diagonal stiffness matrix $\mathbb{K}_i$, and the 3×3 block diagonal surface matrix $\mathbb{S}_{il}$ are defined by their respective diagonal blocks:

$$\begin{cases} (\widetilde{\mathbb{M}}_i^m)_{jk} = (\Phi_{ij}^m, \Phi_{ik}^m)_{K_i}, \quad \text{of size} \quad d_i \times d_i, \quad 1 \leq m \leq 3, \\ (\widetilde{\mathbb{K}}_i^m)_{jk} = \frac{1}{2}((\Phi_{ij}^m, \mathrm{curl}\Phi_{ik}^m)_{K_i} + (\mathrm{curl}\Phi_{ij}^m, \Phi_{ik}^m)_{K_i}), \quad \text{of size} \quad d_i \times d_i, \quad 1 \leq m \leq 3 \\ (\widetilde{\mathbb{S}}_{il}^m)_{jk} = \langle \Phi_{ij}^m, \Phi_{lk}^m \times \mathbf{n}_{il} \rangle_{F_{il}}, \quad \text{of size} \quad d_i \times d_l, \quad l \in \nu_i, \quad 1 \leq m \leq 3, \end{cases}$$

here, d_l denotes the number of DOFs on face $l \in \nu_i$.

Space-discrete formulation

Remark 1. For a metallic boundary face $F_{ij} \in \Gamma_m \cap F_h^B$, the metallic boundary condition is $\mathbf{E}_{h|F_{ij}} = 0$. We therefore define

$$\mathbf{E}_{j|F_{ij}} = -\mathbf{E}_{i|F_{ij}}, \quad \mathbf{H}_{j|F_{ij}} = \mathbf{H}_{i|F_{ij}}. \tag{9}$$

For an absorbing boundary face $F_{ij} \in \Gamma_a \cap F_h^B$, we can define

$$\begin{cases} \mathbf{E}_{j|F_{ij}} = z_i N_{ij} \mathbf{H}_{i|F_{ij}} + \mathbf{E}^{inc}_{i|F_{ij}} - z_i N_{ij} \mathbf{H}^{inc}_{i|F_{ij}}, \\ \mathbf{H}_{j|F_{ij}} = -z_i^{-1} N_{ij} \mathbf{E}_{i|F_{ij}} + \mathbf{H}^{inc}_{i|F_{ij}} + z_i^{-1} N_{ij} \mathbf{E}^{inc}_{i|F_{ij}}, \end{cases} \tag{10}$$

where $N_{ij} = \begin{pmatrix} 0 & n_{ijz} & -n_{ijy} \\ -n_{ijz} & 0 & n_{ijx} \\ n_{ijy} & -n_{ijx} & 0 \end{pmatrix}$, and $\mathbf{E}^{inc}_{i|F_{ij}}$, $\mathbf{H}^{inc}_{i|F_{ij}}$ are given incident fields.

Space-discrete formulation

For all element, we can get a descriptor system of first order in time for (8) as following:

$$\begin{cases} \mathbb{M}\frac{d\underline{\mathbf{H}}_h}{dt} = -\mathbb{K}\underline{\mathbf{E}}_h + \mathbb{S}^i\underline{\mathbf{E}}_h + \mathbb{S}^e\underline{\mathbf{E}}_h + \mathbb{B}^h u_h(t), \\ \varepsilon_\infty \mathbb{M}\frac{d\underline{\mathbf{E}}}{dt} = \mathbb{K}\underline{\mathbf{H}}_h - \mathbb{S}^i\underline{\mathbf{H}}_h - \mathbb{S}^h\underline{\mathbf{H}}_h - \mathbb{M}\underline{\mathbf{J}}_h + \mathbb{B}^e u_e(t), \\ \frac{d\underline{\mathbf{J}}_h}{dt} = -\gamma_d\underline{\mathbf{J}}_h + \omega_d^2\underline{\mathbf{E}}_h. \end{cases} \tag{11}$$

The descriptor system of first order in time can then be written as:

$$\begin{cases} M\dot{x}(t) = Kx(t) + bu(t), \\ y(t) = p^T x(t), \end{cases} \tag{12}$$

with initial condition $x(0) = x_0 = [\mathbf{E}_0(x), \mathbf{H}_0(x), \mathbf{J}_0(x)]^T$, where M, $K \in R^{N\times N}$, p, $b \in R^N$, and $N = 9N_{dof}$.

Outline

1 Introduction
- Model Problem
- Motivation
- Model order reduction

2 DGTD formulations
- Weak variation
- Space-discrete formulation

3 Reduced-order DG formulations
- POD-DGTD formulations
- Krylov subspace based solver
  - Krylov-subspace based operator exponential approach
  - Krylov-subspace based Padé approximation approach

4 Numerical experiments
- Artificial validation case
- Scattering of a plane wave by a Au-nanowire

5 Summary

POD-DGTD formulations

Let

$$W = [x(t_{n_1}), x(t_{n_2}), \cdots, x(t_{n_\ell})] \in R^{N \times \ell}$$

be a collection of **snapshots** of the solution of (12). We compute the singular value decomposition and truncate depending on how fast the singular values decay:

$$W = U\Sigma V^T \approx U_n \Sigma_n V_n^T, \quad n \leq r \leq \ell \ll N.$$

Here, $r = \mathrm{rank}(W)$, U and V are $N \times N$ and $\ell \times \ell$ unitary matrices. Let $U = (\psi_1, \psi_2, \cdots, \psi_N)$ and $V = (\phi_1, \phi_2, \cdots, \phi_\ell)$, then the POD reduced basis is the set $U_n = \{\psi_i\}_{i=1}^n (n \leq r)$.

POD-DGTD formulations

Then considering the approximation of the state vector $x(t)$ by another state vector, constrained to stay in the subspace spanned by the columns of U_n, namely,

$$x(t) \approx U_n z(t), \quad z(t) \in R^n,$$

yields an linear system with respect to the state variable $z(t)$:

$$\begin{cases} MU_n \dot{z}(t) = KU_n z(t) + bu(t), \\ \widetilde{y}(t) = p^T U_n z(t). \end{cases}$$

After left-multiplying the first equation by U_n,we have

$$\begin{cases} U_n^T MU_n \dot{z}(t) = U_n^T KU_n z(t) + U_n^T bu(t), \\ \widetilde{y}(t) = p^T U_n z(t). \end{cases}$$

Then an n th reduced-order model of the linear system (12) in the time domain is naturally defined, and the quadruples (M_n, K_n, b_n, p_n^T) can be simply expressed as $(U_n^T MU_n, U_n^T KU_n, U_n^T b, p^T U_n)$.

POD-DGTD formulations

Remark 2. For the discrete scheme (8), the number of DOFs ($9N_{dof}$) is very large, but the number DOFs n of the POD-DGTD formulations (22) is very small as we will show from the numerical results.

Remark 3. The choice of the dimension d of the POD basis is not obvious. We denote by $\varepsilon(\psi_1, \psi_2, \cdots, \psi_d) = \sum_{j=d+1}^{r} \lambda_j$ the POD energy or error in the POD basis. If we want the POD energy to be less than some prescribed tolerance ρ, i.e., that

$$\varepsilon(\psi_1, \psi_2, \cdots, \psi_n) \leq \rho,$$

we can choose d to be the minimum of positive integer such that

$$\pi(n) = \frac{\sum_{j=1}^{n} \lambda_j}{\sum_{j=1}^{r} \lambda_j} \geq 1 - \rho. \tag{13}$$

Outline

1 Introduction
- Model Problem
- Motivation
- Model order reduction

2 DGTD formulations
- Weak variation
- Space-discrete formulation

3 Reduced-order DG formulations
- POD-DGTD formulations
- Krylov subspace based solver
  - Krylov-subspace based operator exponential approach
  - Krylov-subspace based Padé approximation approach

4 Numerical experiments
- Artificial validation case
- Scattering of a plane wave by a Au-nanowire

5 Summary

Krylov-subspace based operator exponential approach

Introducing the system matrix A as

$$A = -M^{-1}K,$$

stable field approximations can be computed as [Zimmerling J, Wei L, Urbach P, et al, JCP, 2016]

$$x(t) = u(t) * 2\eta(t)Re[\eta(A)exp(-At)M^{-1}b] \quad \text{for } t > 0,$$

where $\eta(t)$ is the Heaviside unit step function. The central approximation of the Krylov subspace techniques described then reads as

$$exp(-At)M^{-1}b = V_n exp(-H_n t)\mathbf{e}_1,$$

$\mathbf{e}_1$ being a first unit basis vector, n being the dimensional of the reduced order system, and V_n, H_n can be obtained by Arnoldi-process or rational Lanczos-process.

The references for Krylov-subspace based operator exponential approach:

- Zimmerling J, Wei L, Urbach P, et al. A Lanczos model-order reduction technique to efficiently simulate electromagnetic wave propagation in dispersive media. Journal of Computational Physics, 2016, 315: 348-362.
- Botchev M A. Krylov subspace exponential time domain solution of Maxwells equations in photonic crystal modeling. Journal of computational and applied mathematics, 2016, 293: 20-34.
- Druskin V, Lieberman C, Zaslavsky M. On adaptive choice of shifts in rational Krylov subspace reduction of evolutionary problems. SIAM Journal on Scientific Computing, 2010, 32(5): 2485-2496.
- ...

Padé approximation and moment-matching

Taking a Laplace transform for the descriptor system (12), assuming zero initial conditional, and then we obtain the following frequency domain formulation of (12):

$$\begin{cases} sMX(s) = KX(s) + bU(s), \\ Y(s) = p^T X(s) \end{cases} \tag{14}$$

where $X(s)$, $Y(s)$, and $U(s)$ respectively denotes the Laplace transform of $x(x)$, $y(x)$, and $u(x)$. Eliminating $X(s)$ in (14) leads to a transfer function of the original system (12) as

$$H(s) = \frac{Y(s)}{U(s)} = p^T(sM - K)^{-1}b, \tag{15}$$

where $s \in \mathbb{C}$, and $H(s) \in R_{N-1,N}$ is a scalar rational function.

Padé approximation and moment-matching

The Taylor series expansion of $H(s)$ about $s_i \in \mathbb{C}$ $(i = 1, 2, \cdots, l)$ is given by

$$H(s) = \sum_{j=0}^{\infty} m_j(s_i)(s - s_i)^j, \tag{16}$$

where $m_j(s_i) = p^T[-(s_i M - K)^{-1} M]^j (s_i M - K)^{-1} b$ are called moments about s_i, l is the number of expansion points. We seek a reduced order system such that the Taylor expansion of the corresponding transfer function at s_i has the form

$$H_n(s) = \sum_{j=0}^{\infty} \widehat{m}_j(s_i)(s - s_i)^j, \tag{17}$$

where $\widehat{m}_j(s_i)$ are called moments about s_i for a reduced order system.

Padé approximation and moment-matching

The function $H_n(s) \in R_{n-1,n}$ is said to be an nth multi-point Padé approximation of $H(s)$ about the expansion point s_i $(i = 1, 2, \cdots, l)$ if it matches with the moments of $H(s)$ as far as possible, i.e.

$$m_j(s_i) = \widehat{m}_j(s_i), \quad j = 0, 1, 2, \cdots, j_i - 1, \quad i = 1, 2, \cdots, l,$$

where $j_i > 0$ denotes the number of the moments corresponding at s_i, and $n = \sum_{i=1}^{l} j_i$. Then,

$$H(s) = H_n(s) + \sum_{j=j_i}^{\infty} (m_j(s_i) - \widehat{m}_j(s_i))((s - s_i)^j), \tag{18}$$

where the last summation term denotes the error between the frequency response of the original system and that of the reduced-order system. If $l = 1$, (17) is a standard nth Padé approximant for $H(s)$.

Padé approximation and moment-matching

If the transfer function $H_n(s)$ of the reduced-order system is expressed as a scalar rational function

$$H_n(s) = \frac{P_{n-1}(s)}{Q_n(s)}, \tag{19}$$

where the numerator $P_{n-1}(s)$ and the denominator $Q_n(s)$ are defined respectively

$$\begin{cases} P_{n-1}(s) = \sum_{j=0}^{n-1} a_j (s-s)^j, \\ Q_n(s) = 1 + \sum_{j=1}^{n} b_j (s-s)^j, \end{cases}$$

and the coefficients $\{a_j\}$ and $\{b_j\}$ are unknown, we can obtain a total of $2n$ linear equations by (18) and (19) by collecting the coefficients of the polynomials. Unfortunately, the coefficient matrix of the linear equations, which is called the Hanker matrix, usually is ill-conditioned.

Padé via Lanczos ($l = 1, s0$)

For the matrix $B = -(K - s_0 M)^{-1} M$, the vector $r = (K - s_0 M) b$, and a left staring vector p, the nth Krylov subspace $\mathcal{K}_n(B, r)$ is spanned by a sequence of n column vectors:

$$\mathcal{K}_n(B, r) = span\{r, Br, B^2 r, \cdots, B^{n-1} r\}.$$

This is sometimes called the right Krylov subspace. When the matrix B is nonsymmetric, there is a left Krylov subspace generated by B^T and a starting vector p defined by

$$\mathcal{K}_n(B^T, p) = span\{p, B^T p, (B^T)^2 p, \cdots, (B^T)^{n-1} p\}.$$

Note that the first $2n$ moments m_i of $H(s)$ are connected with Krylov subspaces through computing the inner products between the left and right Krylov sequences:

$$m_{2i} = ((B^T)^i p)^T \cdot (B^i b)^T, \quad m_{2i+1} = ((B^T)^i p)^T \cdot (B^{i+1} b)^T,$$

for $i = 1, 2, \cdots, n-1$.

Padé via Lanczos

The left and right Krylov subspaces contain the desired information of moments, but the vectors $B^i r$ and $(B^T)^i p$ are unsuitable as basis vectors. The remedy is to construct more suitable basis vectors $\{v_1, v_2, \cdots, v_n\}$ and $\{w_1, w_2, \cdots, w_n\}$ such that they span the same desired Krylov subspaces. It is well-known that the Lanczos process is an elegant way to generate the desired basis vectors.

Lanczos process

Give a matrix B, a right staring vector r and a left staring vector p, the Lanczos process generates the basis vector $\{v_i\}$ and $\{w_i\}$, known as the Lanczos vector. Moreover, these Lanczos vector are constructed to be biorthogonal

$$(w_j)^T v_k = 0, \quad \text{for all} \quad j \neq k.$$

The Lanczos vectors can be generated by two three-term recurrences. There recurrences can be stated compactly in matrix form as follows

$$\begin{cases} BV_n = V_n T_n + \rho_{n+1} v_{n+1} \mathbf{e}_n^T, \\ B^T W_n = \widetilde{V}_n T_n + \eta_{n+1} w_{n+1} \mathbf{e}_n^T, \end{cases}$$

where T_n and $\widetilde{T}_n$ are the tridiagonal matrices.

Reduced Order Model

In general, the application of model order reduction to (12) yields a reduced order model by using the orthogonal projection $x(t) = V_n z(t)$

$$\begin{cases} M_n \dot{z}(t) = K_n z(t) + b_n u(t), \\ \widetilde{y}(t) = p_n^T z(t), \end{cases} \tag{20}$$

where $M_n,\ K_n \in R^{n\times n}$, and $b_n,\ p_n \in R^n$ have a significantly smaller dimension $n \ll N$ than the original system (12), and

$$M_n = V_n^T M V_n, \quad K_n = V_n^T K V_n, \quad b_n = V_n^T b, \quad p_n = V_n^T p.$$

Why is the simple choice $l = 1$, $s_1 = s_0$?

- If $l > 1$, $s_i \in \mathbb{C}$ $(i = 1, 2, \cdots, l)$, e.g, the rational Arnoldi method, the selection of suitable expansion points (also called shifts) is crucial for the quality of the resulting reduced order model.
- If $l = 1$, $s_1 = \mathit{infinit}$, e.g, PVL with expansion at infinity is fast while the accuracy of the method is very low.

Outline

1 Introduction
- Model Problem
- Motivation
- Model order reduction

2 DGTD formulations
- Weak variation
- Space-discrete formulation

3 Reduced-order DG formulations
- POD-DGTD formulations
- Krylov subspace based solver
  - Krylov-subspace based operator exponential approach
  - Krylov-subspace based Padé approximation approach

4 Numerical experiments
- Artificial validation case
- Scattering of a plane wave by a Au-nanowire

5 Summary

Information about test problems:

- The computational domain: the square $\Omega_{\square} = (x, y) \in [0, l] \times [0, l]$.
- The boundary condition: PEC.
- The Drude parameters: $\varepsilon_{\infty} = 3.7362$, $\omega_d = 1.3871e7$ GHz, $\gamma_d = 4.41544e4$ GHz.
- Codes: MATLAB 2013b (Memory: 8Gb).
- Method: DG methods with RK_4, PVL-DGTD methods.

Table: Convergence results for the dispersive cavity problem.

	DGTD-$\mathbb{P}_1$		DGTD-$\mathbb{P}_2$		DGTD-$\mathbb{P}_3$		DGTD-$\mathbb{P}_4$	
h	L^2-error	r	L^2-error	r	L^2-error	r	L^2-error	r
3.678e-08	3.482e-08	-	9.364e-10	-	4.161e-11	-	6.735e-13	-
1.839e-08	1.618e-08	**1.106**	1.965e-10	**2.253**	5.140e-12	**3.017**	4.091e-14	**4.042**
9.194e-09	7.931e-09	**1.028**	4.678e-11	**2.070**	6.448e-13	**2.995**	2.585e-15	**3.984**
4.597e-09	3.946e-09	**1.007**	1.161e-11	**2.011**	8.099e-14	**2.993**	1.644e-16	**3.975**

It can be seen that the convergence order of numerical simulation is to satisfy the theoretical convergence order.

Table: Computational performance of the artificial problem.

	DGTD		PVL-DGTD		
Mesh	N	L^2-error	n	s_0	L^2-error
		$\mathbb{P}_1$			
M1	3744	3.482e-08	25	$1300f$	3.489e-08
M2	14976	1.618e-08	25	$2100f$	1.618e-08
M3	59904	7.931e-09	35	$3500f$	7.930e-09
		$\mathbb{P}_2$			
M1	7488	9.364e-10	35	$1700f$	9.366e-10
M2	29952	1.965e-10	35	$3700f$	1.964e-10
M3	119808	4.678e-11	90	$12000f$	4.684e-11
		$\mathbb{P}_3$			
M1	12480	4.161e-11	45	$1500f$	4.162e-11
M2	49920	5.140e-12	75	$3100f$	5.799e-12
M3	199680	6.448e-13	100	$15000f$	6.518e-13
		$\mathbb{P}_4$			
M1	18720	6.735e-13	52	$2100f$	6.907e-13
M2	74880	4.092e-14	90	$10000f$	4.292e-14
M3	299520	2.585e-15	150	$20000f$	3.473e-15

✓ the difference between the error calculated by the DGTD method and that calculated by the PVL-DGTD is small.

✓ while the dimension of the reduced order model is much smaller than that of the original system.

Table: Computational performance of the artificial problem.

Mesh	DGTD $T_{\text{construction}}$(s)	DGTD T_{solution}(s)	PVL-DGTD $T_{\text{construction}}$(s)	PVL-DGTD T_{PVL}(s)	PVL-DGTD T_{solution}(s)	Speed-up
			$\mathbb{P}_1$			
M1	0.566	0.405	0.566	0.148	0.026	57.037%
M2	2.535	3.135	2.535	0.990	0.091	65.518%
M3	14.499	29.041	14.499	9.137	1.550	63.200%
			$\mathbb{P}_2$			
M1	0.601	3.109	0.601	0.613	0.059	78.385%
M2	2.873	28.020	2.873	3.725	0.437	85.146%
M3	22.994	285.670	22.994	58.094	8.376	76.732%
			$\mathbb{P}_3$			
M1	0.638	10.680	0.638	2.623	0.147	74.064%
M2	3.765	115.400	3.765	23.464	2.232	77.733%
M3	52.804	1135.300	52.504	224.765	28.818	77.664%
			$\mathbb{P}_4$			
M1	0.896	36.593	0.896	7.689	0.360	78.004%
M2	7.155	334.265	7.155	92.095	4.832	71.003%
M3	126.198	3148.400	126.198	783.482	74.960	72.734%

✓ It is seen that the PVL-DGTD method saves the required CPU time to yield a uniform accuracy level.

- The point with coordinates: (4.560e-8, 6.625e-7);
- Methods: DGTD-$\mathbb{P}_2$ with M2, PVL-DGTD-$\mathbb{P}_2$ with M2.

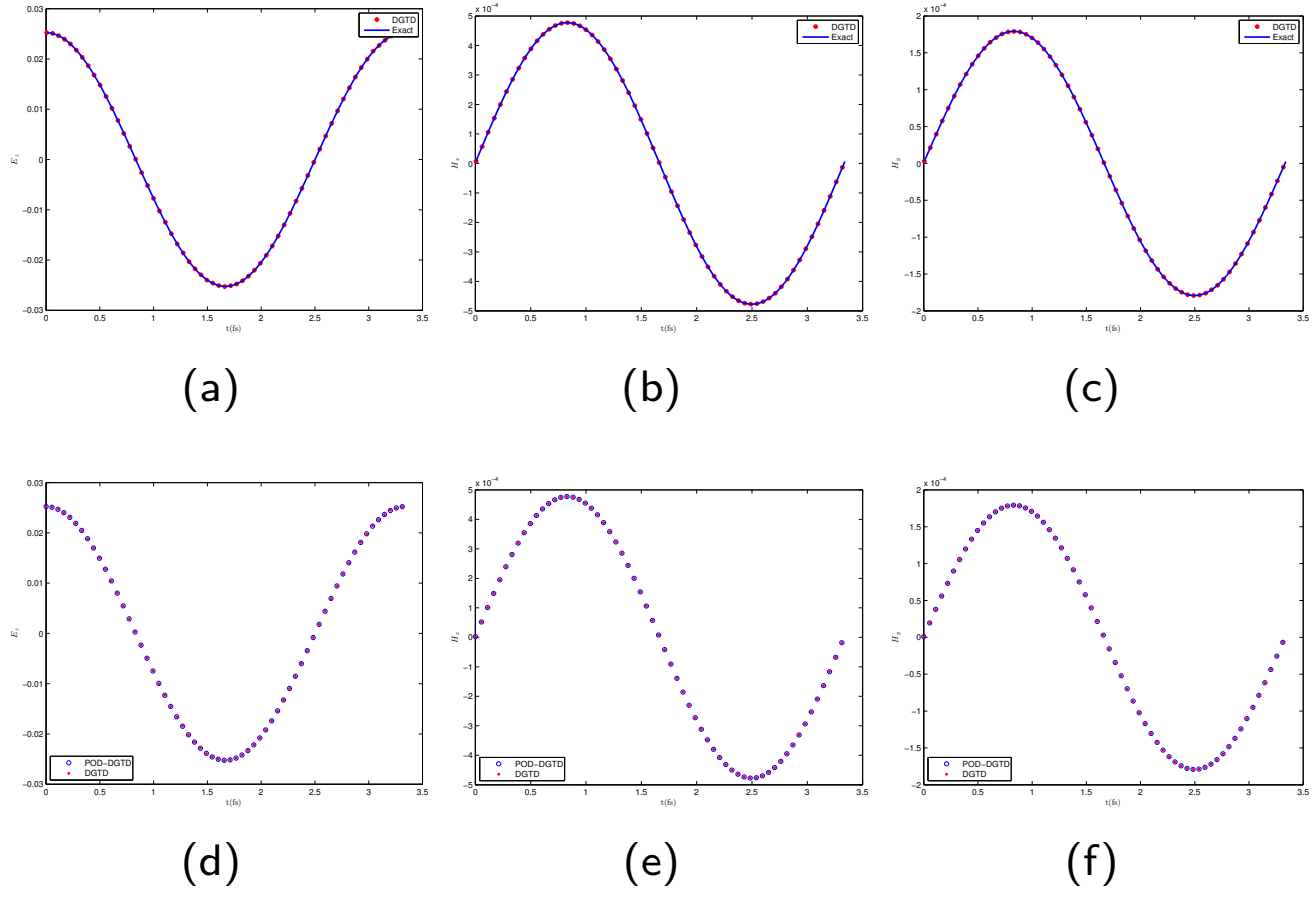

Figure: Comparisons between the usual DGTD methods and the PVL-DGTD methods. (a)∼(c): the usual DGTD solutions for E_z, H_x, H_y. (d)∼(f): the PVL-DGTD solutions for E_z, H_x, H_y.

- Time: t = 1e-6;

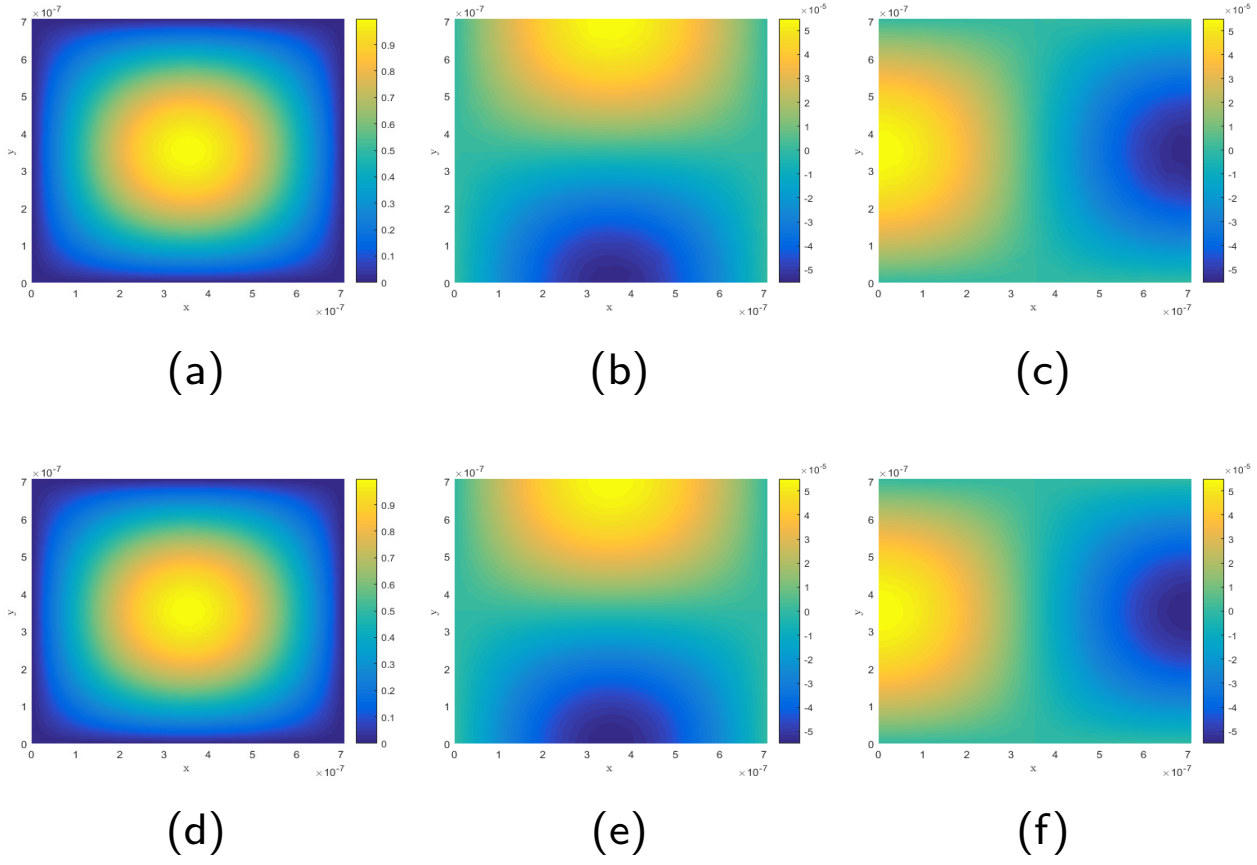

Figure: Comparisons between the usual DGTD methods and the PVL-DGTD methods. (a)∼(c): the DGTD solutions for E_z, H_x, H_y. (d)∼(f): the PVL-DGTD solutions for E_z, H_x, H_y.

✓ We again find that PVL-DGTD solutions coincide with the DGTD solutions and the analytical solutions.

Outline

1 Introduction
- Model Problem
- Motivation
- Model order reduction

2 DGTD formulations
- Weak variation
- Space-discrete formulation

3 Reduced-order DG formulations
- POD-DGTD formulations
- Krylov subspace based solver
  - Krylov-subspace based operator exponential approach
  - Krylov-subspace based Padé approximation approach

4 Numerical experiments
- Artificial validation case
- Scattering of a plane wave by a Au-nanowire

5 Summary

Information about test problems:

- The computational domain: a gold disk of radius $r = 2nm$.
- The boundary condition: ABC, and propagating along the $-y$ axis.
- The incident plane wave (a sinusoidal modulated Gaussian polse):

$$\{E_x^{inc}, H_z^{inc}\} \propto \sin(2\pi f_c(t-\tau))\exp(-(\frac{t-\tau}{\alpha})^2).$$

- The Drude parameters: $\varepsilon_\infty = 1$, $\omega_d = 1.19e4$ THz, $\gamma_d = 141$ THz;
- Codes: MATLAB 2013b (Memory: 8Gb).

Table: Comparisons between the DGTD solutions and the POD-DGTD solutions on CPU times and errors for Au-nanowire.

		Usual DG(a)	Reduced-order DG(b)	Gain	$\max_{n\in[0,N_t]} e_d^n$
MS	$\mathbb{P}_p$	CPU time(s)	CPU time(s)	$\mathrm{CPU}_a/\mathrm{CPU}_b$	
	1	4.253	**0.238**	17.906	7.431e-12
M1	2	15.637	**0.579**	27.007	5.028e-12
	1	26.990	**1.494**	18.070	4.824e-12
M2	2	118.545	**5.222**	22.703	1.368e-12
	1	866.590	**14.744**	58.774	8.324e-13
M3	2	3496.236	**43.743**	79.926	5.531e-13

- Field distributions. Time: $t = (6*(1e\text{-}16))$.

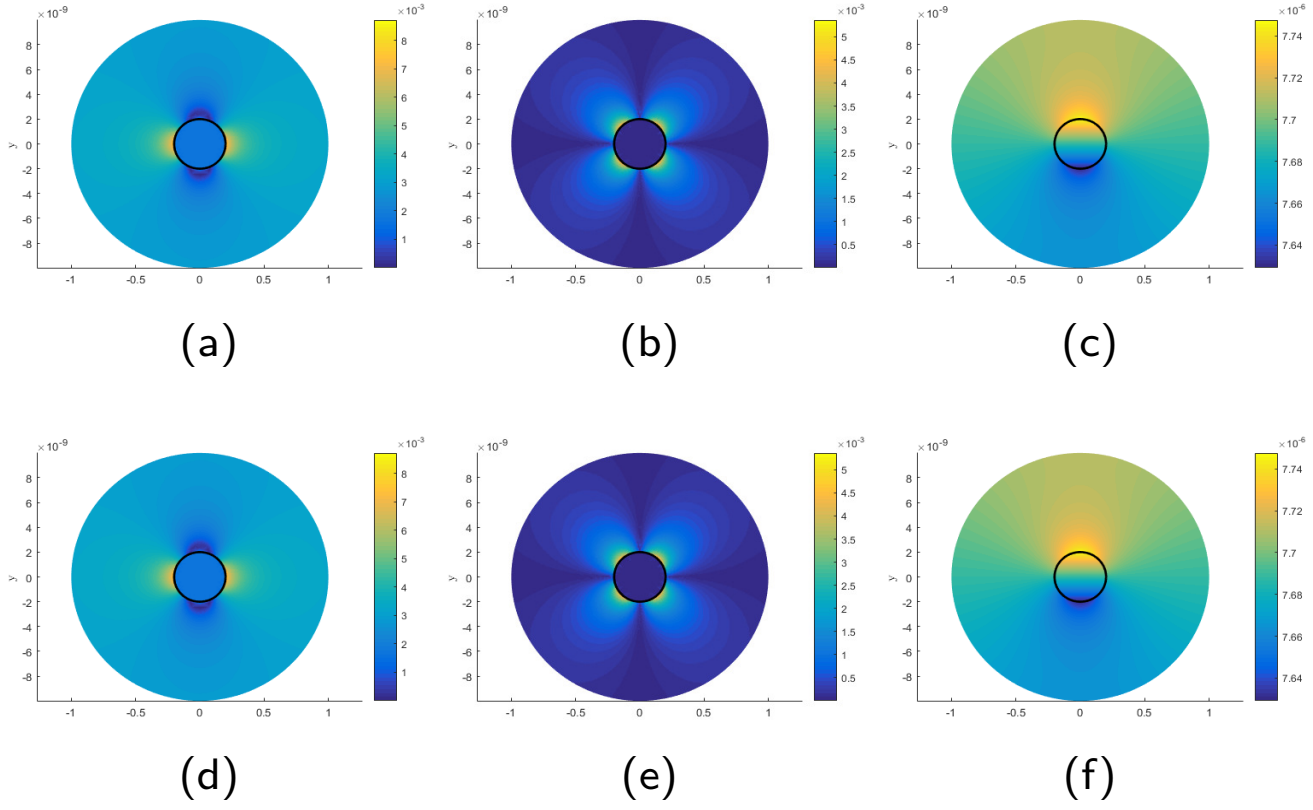

Figure: Field distributions for the simulation of the scattering a plane wave by a gold nanowire. We plot the contour lines of the fields in frequency domain, i.e. the fields are calculated by a DFT from the time-domain solutions by DGTD and POD-DGTD methods. (a)$\sim$(c): the DGTD solutions for E_x, E_y, H_z. (d)$\sim$(f): the POD-DGTD solutions for E_x, E_y, H_z.

- Field distributions: E_x.
- Time: t = (6*(1e-16)).

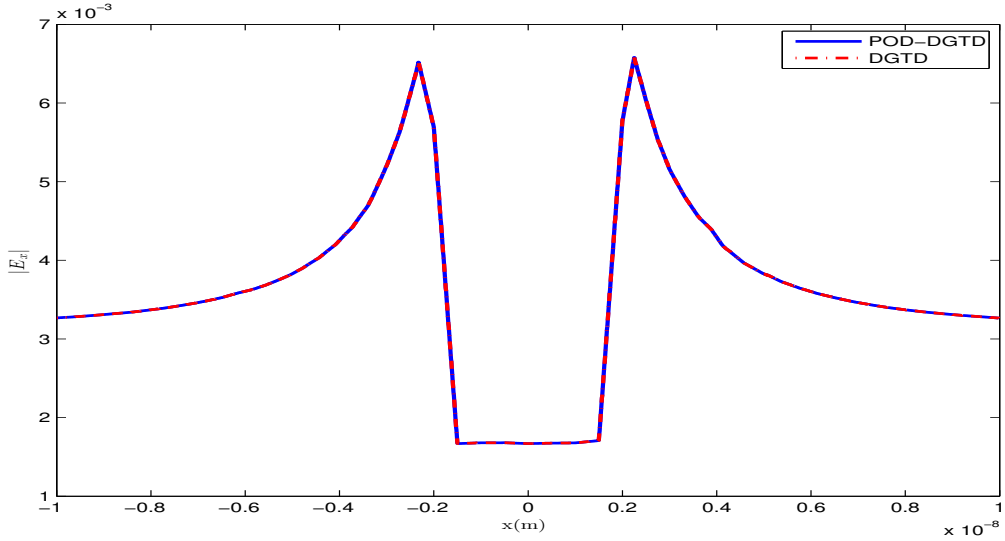

Figure: 1D distribution along the x for the modulus of E_x in the Fourier domain.

Conclusions and Future works

Conclusions:

Conclusions and Future works

Conclusions:

- The reduced-order DG method is developed for saving time;
- The reduced-order DG method has less degrees of freedom compared to the usual DG method;
- Numerical results show their advantages.

Conclusions and Future works

Conclusions:

- The reduced-order DG method is developed for saving time;
- The reduced-order DG method has less degrees of freedom compared to the usual DG method;
- Numerical results show their advantages.

Future works:

Conclusions and Future works

Conclusions:

- The reduced-order DG method is developed for saving time;
- The reduced-order DG method has less degrees of freedom compared to the usual DG method;
- Numerical results show their advantages.

Future works:

- More complex 3d realistic applications should be investigated;
- The error bounds between the usual DG solutions and the reduced-order DG solutions will be derived;
- The extension of this reduce-order method to more general physical model, e.g., Hydrodynamic Drude and generalized non-local modes.
- other MOR methods, such as, rational Krylov subspace technique.

References I


K. Li, T.-Z. Huang, L. Li, L. Stéphane,
A reduced-order discontinuous Galerkin element formulation based on POD method for the time-domain Maxwell's equations in dispersive media.


K. Li, T.-Z. Huang, L. Li, L. Stéphane,
A Krylov subspace based solver for discontinuous Galerkin element approximation of time-domain Maxwell's equations in dispersive media.